applied sciences

MDPI

Article

Structural Damage Localization under Unknown Seismic Excitation Based on Mahalanobis Squared Distance of Strain Transmissibility Function

Lijun Liu *, Xin Zhang, Ying Lei and Zhupeng Zheng

Department of Civil Engineering, Xiamen University, Xiamen 361005, China; 25320191151814@stu.xmu.edu.cn (X.Z.); ylei@xmu.edu.cn (Y.L.); xpeng@xmu.edu.cn (Z.Z.)
* Correspondence: liulj214@xmu.edu.cn; Tel.: +86+153-0692-7166

Abstract: Due to the unpredictability of seismic excitation, the data-driven damage identification method, which only depends on the monitoring response data, has a good development prospect in structural health monitoring. In recent years, damage identification methods based on transmissibility function (TF) and Mahalanobis squared distance (MSD) have been widely studied. However, the existing methods are only applicable to damage warning. To overcome this limitation, an improved method for structural damage localization is proposed. Strain TF is used to eliminate the influence of unknown ambient excitation and unknown seismic excitation, which is more sensitive to local damage than traditional TF based on acceleration and displacement data. The MSD of strain TF is employed to construct a novel damage indicator that is used to identify the damage location. Two numerical simulations have been conducted to verify the feasibility of the method for damage localization and good anti-noise performance. In the case of the multi-damage condition, the novel damage indicator is performed to estimate the severity of damage to some extent.

Keywords: damage localization; strain transmissibility function; mahalanobis squared distance; ambient excitation; unknown seismic excitation; data-driven method

check for updates

Citation: Liu, L.; Zhang, X.; Lei, Y.; Zheng, Z. Structural Damage Localization under Unknown Seismic Excitation Based on Mahalanobis Squared Distance of Strain Transmissibility Function. *Appl. Sci.* **2022**, *12*, 3115. https://doi.org/10.3390/app12063115

Academic Editor: Jun-Bao Li

Received: 16 February 2022
Accepted: 16 March 2022
Published: 18 March 2022

1. Introduction

Bridge structures may be damaged or even destroyed in earthquake disasters. Therefore, many large bridges have been equipped with long-term structural health monitoring (SHM) systems for structural safety. Since the seismic excitations are unpredictable, it is still a great challenge to use only the monitoring data to evaluate the state of the structure, detect and localize the abnormal characteristics of structures, and evaluate and extend the service life of the structure [1–4].

Data-driven damage detection has become one of the most popular methods in SHM. It does not need external excitations and only relies on the monitoring data of responses [5]. Since the transmissibility function (TF) reflects the response transfer characteristics of the structure and does not need the information of the external excitation, TF-based methods have attracted more attention in the field of SHM. Because of its advantages, TF is mainly applied to three categories of SHM system: modal analysis [6–8], damage detection [9,10], and model updating [11,12]. In addition, in recent years, TF has been widely used in vibro-acoustics for transfer path analysis [13,14], force identification or reconstruction [15,16], and characterization of the dynamic behavior of vibration isolation systems [17]. This paper mainly studies the application of TF in damage identification.

Many scholars used TF to construct various damage indicators for damage identification. Maia et al. [18,19] proposed a response vector assurance criterion (RVAC) and a relative damage quantification indicator (DRQ) with transmissibility. Zhou et al. [20–23] proposed a variety of damage indicators based on TF and combined the concepts of coherence function (ATC/TMAC), similarity measure (CI/MAC), and correlation analysis (CDI) to determine the occurrence of damage. Diao et al. [24] proposed a new damage indicator based on the TF and studied the damage localization of the offshore platform structure support. Al-Jailawi et al. [25] also established an indicator to compare the advantages and disadvantages of the angular velocity TF and the acceleration TF on damage localization. Cheng et al. [26] studied the mechanism of damage localization using TF to establish the corresponding damage indicator. Yu et al. [27,28] proposed a structural damage identification strategy based on the weighted transmissibility assurance criterion. In addition, some literature combined TF and a distance measure to construct damage indicators, which is an outlier analysis, such as Cosh distance, Euclidean distance, Mahalanobis squared distance (MSD), Itakura distance, City Block distance, Chebyshev distance, and Minkowski distance [29–35].

Due to its good applicability and sensitivity to damage, MSD has been widely used in structural damage identification [36]. Some scholars studied MSD by calculating the TF of all measuring points at a certain frequency point as the test vector and detecting damage by the MSD vector varying with the frequency point [29–31]. Chen et al. [32] and Zhou et al. [33] formed the TF matrix by considering the responses of all measuring points, used the principal component analysis to reduce the dimension, and detected the damage based on MSD. Fan et al. [34] only used the acceleration response time history of two measuring points to obtain the wavelet TF and judged whether the observation value of the unknown state was an abnormal value according to MSD. Xu et al. [35] grouped the TFs before and after damage and constructed the TF matrix. Then, the principal components were extracted by principal component compression. Moreover, the MSD between the principal components before and after structural damage was calculated, which was used as the sample of statistical analysis. Finally, the statistics were constructed, and the damage identification was studied by *t*-test. However, the above-mentioned methods combining TF and distance measure are only used to detect the occurrence of damage, but not damage location. In addition, TF is calculated by acceleration and displacement response in the previous studies, while there is little research on TF based on strain response. Structural strain response is a local characteristic of the structure. When the structure near the strain gauge is damaged, the strain response recorded by the strain gauge will change significantly. Since strain TF is more sensitive to damage than traditional TF [37], it is applied to structural damage identification in this paper.

To overcome the above limitations, an improved method for identifying the structural damage location under unknown seismic excitation using TF and MSD is proposed in this paper. Firstly, strain TF is used to eliminate the influence of unknown ambient excitation and unknown seismic excitation, which is more sensitive to local damage than traditional TF based on acceleration and displacement data. Then, the strain TF observation matrix in the intact structure under ambient excitations is obtained, and the MSD threshold is determined to judge outliers. Finally, the strain TF test vector in the test structure under unknown seismic excitation is obtained to calculate MSD between the test structure and the baseline, which is compared with the threshold to identify the structural damage location. To verify the effectiveness of this method, numerical simulations of a simply supported beam and a cable-stayed bridge were carried out. All simulation results show that the proposed method reveals quite a significant capacity for accurately locating structural damage, identifying the degree of damage to a certain extent, and showing good noise resistance to small damage.

The remainder of this paper is as follows. In Section 2, the strain TFs of unknown ambient excitation under normal operating conditions and unknown seismic excitation under damage conditions are analyzed. In Section 3, the damage localization based on MSD of strain TFs is discussed. In Section 4, the numerical examples of a simply supported beam and a cable-stayed bridge are provided to demonstrate the accuracy of the method. In Section 5, there are some conclusions and future work directions.

2. The Strain Transmissibility Function (TF)

2.1. The Strain TF of the Intact Structure under Unknown Ambient Excitation

Transmissibility function (TF) is defined as the Fourier transform or the spectrum ratio of two measurement responses. For an n-DOFs structure subject to unknown ambient excitation $\boldsymbol{P} = [P_1, P_2, \ldots, P_m]^{\mathrm{T}}$, the basic motion equation is as follows:

$$\boldsymbol{M}\ddot{\boldsymbol{x}}(t) + \boldsymbol{C}\dot{\boldsymbol{x}}(t) + \boldsymbol{K}\boldsymbol{x}(t) = \boldsymbol{I}\boldsymbol{P}(t) \tag{1}$$

where $\boldsymbol{M}$, $\boldsymbol{C}$, and $\boldsymbol{K}$ represent the mass, damping, and stiffness matrices of the structural system, respectively; $\ddot{\boldsymbol{x}}(t)$, $\dot{\boldsymbol{x}}(t)$, and $\boldsymbol{x}(t)$ are acceleration, velocity, and displacement response vectors; $\boldsymbol{I}$ is the influence matrix of ambient excitation; $\boldsymbol{P}(t)$ is assumed to be white noise to the intact structure.

In the frequency domain, Equation (1) is transformed as:

$$\boldsymbol{x}(\omega) = \boldsymbol{H}(i\omega)\boldsymbol{I}\boldsymbol{P}(\omega) \tag{2}$$

where $\boldsymbol{H}(i\omega) = \left(\omega^2\boldsymbol{M} + i\omega\boldsymbol{C} + \boldsymbol{K}\right)^{-1}$. Compared with the displacement response, the strain response as a local feature is more sensitive to small deviations. The strain in this study refers to normal strains because the strain gauges only measure normal strains in a certain direction. According to the derivation results in [38], the relationship between displacement and strain is expressed by Equation (3).

$$\varepsilon_e = \boldsymbol{a}_e\boldsymbol{x};\ \boldsymbol{a}_e = \boldsymbol{U}_e\boldsymbol{Y}_e\boldsymbol{W}_e \tag{3}$$

where $\boldsymbol{a}_e$ is the transformation vector, which is described as a $1 \times n$ vector. Furthermore, $\boldsymbol{a}_e$ is viewed as the multiplication of the selection matrix $\boldsymbol{W}_e$, the coordinate system transformation matrix $\boldsymbol{Y}_e$, and the shape function $\boldsymbol{U}_e$.

According to the definition of the TF, the TF is expressed as the spectral ratio of two structural responses of the measurement point *i* and the reference point *j*. Since the power spectral density of white noise is constant, the strain TF under ambient excitation is shown in Equation (4):

$$T^{\varepsilon}_{i,j}(\omega) = \frac{G^{\varepsilon}_{i,j}(\omega)}{G^{\varepsilon}_{j,j}(\omega)} = \frac{\varepsilon_i(\omega)\varepsilon^*_j(\omega)}{\varepsilon_j(\omega)\varepsilon^*_j(\omega)} = \frac{S_0 \sum\limits_{r=1}^{n}\sum\limits_{k=1}^{n}\sum\limits_{f=1}^{m}(a_i)_r H_{rk}(\omega) I_{kf} \sum\limits_{r=1}^{n}\sum\limits_{k=1}^{n}\sum\limits_{f=1}^{m}\left(a_j\right)_r H^*_{rk}(\omega) I_{kf}}{S_0 \sum\limits_{r=1}^{n}\sum\limits_{k=1}^{n}\sum\limits_{f=1}^{m}\left(a_j\right)_r H_{rk}(\omega) I_{kf} \sum\limits_{r=1}^{n}\sum\limits_{k=1}^{n}\sum\limits_{f=1}^{m}\left(a_j\right)_r H^*_{rk}(\omega) I_{kf}} \tag{4}$$

where $G^{\varepsilon}_{i,j}(\omega)$ is the strain cross-power spectrum of the structural responses of point *i* and the reference point *j*; $G^{\varepsilon}_{j,j}(\omega)$ is the strain auto-power spectrum of the reference point *j*; $\varepsilon^*_j(\omega)$ means the complex conjugate of $\varepsilon_j(\omega)$; S_0 is a constant, which is the power spectral density of the excitation; $H_{rk}(\omega)$ is the frequency response function; and $H^*_{rk}(\omega)$ is the complex conjugate of $H_{rk}(\omega)$. From Equation (4), it is noted that $T^{\varepsilon}_{i,j}(\omega)$ is not influenced by the ambient excitations and is only related to the structural characteristics.

2.2. The Strain TF of the Damaged Structure under Unknown Seismic Excitation

For the damaged structure subject to unknown seismic excitation $\ddot{u}_g(t)$, the motion equation is expressed as:

$$\boldsymbol{M}\ddot{\boldsymbol{x}}(t) + \boldsymbol{C}\dot{\boldsymbol{x}}(t) + \boldsymbol{K}\boldsymbol{x}(t) = \boldsymbol{M}\boldsymbol{I}^{(g)}\ddot{u}_g(t) \tag{5}$$

where $\boldsymbol{I}^{(g)}$ denotes the effect vector of seismic excitation $\ddot{u}_g(t)$. Then, according to the relationship between displacement and strain above, the strain TF of measurement point i and reference point j under seismic excitation is calculated as:

$$T_{i,j}^{d\varepsilon}(\omega) = \frac{G_{i,j}^{\varepsilon}(\omega)}{G_{j,j}^{\varepsilon}(\omega)} = \frac{\sum_{r=1}^{n}\sum_{k=1}^{n}\sum_{f=1}^{m}(a_i)_r H_{rk}(\omega) M_{kf} I_f^{(g)} \sum_{r=1}^{n}\sum_{k=1}^{n}\sum_{f=1}^{m}(a_j)_r H_{rk}^{*}(\omega) M_{kf} I_f^{(g)}}{\sum_{r=1}^{n}\sum_{k=1}^{n}\sum_{f=1}^{m}(a_j)_r H_{rk}(\omega) M_{kf} I_f^{(g)} \sum_{r=1}^{n}\sum_{k=1}^{n}\sum_{f=1}^{m}(a_j)_r H_{rk}^{*}(\omega) M_{kf} I_f^{(g)}} \tag{6}$$

As expressed by Equation (6), $T_{i,j}^{d\varepsilon}(\omega)$ is independent of the seismic excitation $\ddot{u}_g(t)$ and only depends on structural characteristics.

3. The Improved Structural Damage Localization Method

To overcome the limitation that existing methods combining TF and distance measure are only used for damage warning, an improved structural damage localization method under unknown seismic excitation is developed in this paper. A new damage indicator on the basis of MSD and strain TF is proposed to identify the damage location.

3.1. Mahalanobis Squared Distance (MSD)

Mahalanobis distance is a concept of distance proposed by Indian statistician P.C. Mahalanobis in 1936. It is used to represent the covariance distance of data and is an effective method to calculate the similarity of two unknown sample sets. Different from Euclidean distance, it considers the relationship between various characteristics and is scale-independent. Therefore, it is used to eliminate the interference of correlation between variables. The definition of Mahalanobis distance is as follows:

$$d^2{}_{MSD} = (\boldsymbol{x} - \overline{\boldsymbol{y}})^{\mathrm{T}} \sum^{-1} (\boldsymbol{x} - \overline{\boldsymbol{y}}) \tag{7}$$

where $\boldsymbol{x}$ is the test vector, $\overline{\boldsymbol{y}}$ is the mean vector of the sample matrix, $\sum^{-1}$ is the inverse covariance matrix of the sample matrix, and the superscript T means transposed.

3.2. Damage Indicator Based on MSD of Strain TF

The strain TF reflects the dynamic characteristics of the structure and is more sensitive to damage than the traditional TF based on acceleration and displacement data. From the vibration characteristics of the structure, it can be seen that a change of the structure state will inevitably lead to a change of the dynamic time-history response, and the TF as the ratio of the structural characteristic parameters will change naturally. Then, the MSD constructed by the strain TF before and after the structural damage will also change. Therefore, the damage indicator based on MSD is defined as:

$$DI_{i,j} = \left(\boldsymbol{T}_{i,j}^{d\varepsilon}(\omega) - \overline{\boldsymbol{Z}}_{i,j}^{\varepsilon}(\omega)\right)^{\mathrm{T}} \sum^{-1} \left(\boldsymbol{T}_{i,j}^{d\varepsilon}(\omega) - \overline{\boldsymbol{Z}}_{i,j}^{\varepsilon}(\omega)\right) \tag{8}$$

where $DI_{i,j}$ is the damage indicator, and $\boldsymbol{T}_{i,j}^{d\varepsilon}(\omega)$ is the strain TF calculated by Equation (6) under unknown seismic excitation in the damaged state. As the test vector of MSD, it is in the form of column vector. $\boldsymbol{Z}_{i,j}^{\varepsilon}$ is the strain TF matrix (the row corresponds to the measured value obtained by applying n times of ambient excitation of different intensity, and the column corresponds to each frequency point) for the baseline (the intact state). $\overline{\boldsymbol{Z}}_{i,j}^{\varepsilon}(\omega)$ is the mean vector at each frequency point, which is expressed as a column vector. The superscript T indicates transposed. $\sum^{-1}$ is the inverse covariance matrix of $\boldsymbol{Z}_{i,j}^{\varepsilon}$. Taking the TF of the second element and the first element (the reference element) as an example, the strain transmissibility function matrix $\mathbf{Z}_{2,1}^{\varepsilon}$, mean vector $\overline{\mathbf{Z}}_{2,1}^{\varepsilon}(\omega)$, and the inverse covariance matrix $\sum^{-1}$ of baseline are as follows.

$$\mathbf{Z}_{2,1}^{\varepsilon} = \begin{bmatrix} Z_{2,1}^{\varepsilon(1)}(\omega_1) & Z_{2,1}^{\varepsilon(1)}(\omega_2) & \dots & Z_{2,1}^{\varepsilon(1)}(\omega_m) \\ Z_{2,1}^{\varepsilon(2)}(\omega_1) & \dots & \dots & \vdots \\ \vdots & \dots & \dots & Z_{2,1}^{\varepsilon(n-1)}(\omega_m) \\ Z_{2,1}^{\varepsilon(n)}(\omega_1) & \dots & Z_{2,1}^{\varepsilon(n)}(\omega_{m-1}) & Z_{2,1}^{\varepsilon(n)}(\omega_m) \end{bmatrix} \tag{9}$$

$$\overline{\mathbf{Z}}_{2,1}^{\varepsilon}(\omega) = mean(\mathbf{Z}_{2,1}^{\varepsilon}) = \begin{bmatrix} \overline{Z}_{2,1}^{\varepsilon}(\omega_1) & \overline{Z}_{2,1}^{\varepsilon}(\omega_2) & \dots & \overline{Z}_{2,1}^{\varepsilon}(\omega_m) \end{bmatrix}^{\mathrm{T}} \tag{10}$$

$$\sum^{-1} = Cov^{-1}(\mathbf{Z}_{2,1}^{\varepsilon}) = \begin{bmatrix} V_{1,1} & V_{1,2} & \dots & V_{1,m} \\ V_{2,1} & \dots & \dots & \vdots \\ \vdots & \dots & \dots & V_{n-1,1} \\ V_{m,1} & \dots & V_{m,m-1} & V_{m,m} \end{bmatrix}^{-1} \tag{11}$$

where

$$V_{p,q} = \frac{1}{n-1}\sum_{k=1}^{n}(Z_{2,1}^{\varepsilon(k)}(\omega_p) - \overline{Z}_{2,1}^{\varepsilon}(\omega_p))(Z_{2,1}^{\varepsilon(k)}(\omega_q) - \overline{Z}_{2,1}^{\varepsilon}(\omega_q)) \tag{12}$$

in which $Z_{2,1}^{\varepsilon(n)}(\omega_m)$ means the strain TF of the second element and the first element at the ω_m frequency point obtained by the n-th measurement. $\overline{Z}_{2,1}^{\varepsilon}(\omega_m)$ represents the average value of the n values at the ω_m point. $V_{p,q}$ is the value of the covariance calculation result in the p-th row and the q-th column of the matrix.

Firstly, the power spectrum of the strain response of the intact structure under ambient excitation is estimated, and the strain TF of two measuring points is calculated as an m-dimensional vector. Next, the m-dimensional vector is observed n times through different intensities of ambient excitation to form an observation matrix with $n \times m$ dimension of sample space. Then, the inverse covariance of the matrix and the mean value for each frequency point are calculated. To judge whether the observed value of the unknown structure state is an outlier, it is necessary to determine a boundary to distinguish the singular value from the normal value, that is, to determine the observation threshold. In this paper, the maximum value of MSD calculated by n measurements of the intact state is selected as the threshold value, namely $\mathrm{MSD}_{\mathrm{max(intact)}}$. After that, the TF calculated from the strain responses of the two measuring points under unknown seismic excitation in the damaged state is used as the test vector of the MSD. In this paper, earthquakes are divided into two categories: main-shocks and after-shocks. The main-shocks are used to induce the bridge earthquake damage, and after-shocks are used to excite the damaged bridges to obtain structural responses [39]. Finally, the $\mathrm{MSD}_{\mathrm{(test)}}$ between each set of test data and the baseline is calculated to compare with the threshold value to identify the damage location of the structure. If the measurement point j is close to the damaged location, the indicator $DI_{i,j}$ of the damaged state will exceed the set threshold, and the damage location can be accurately identified. Figure 1 shows the workflow of damage localization based on MSD of strain TF.

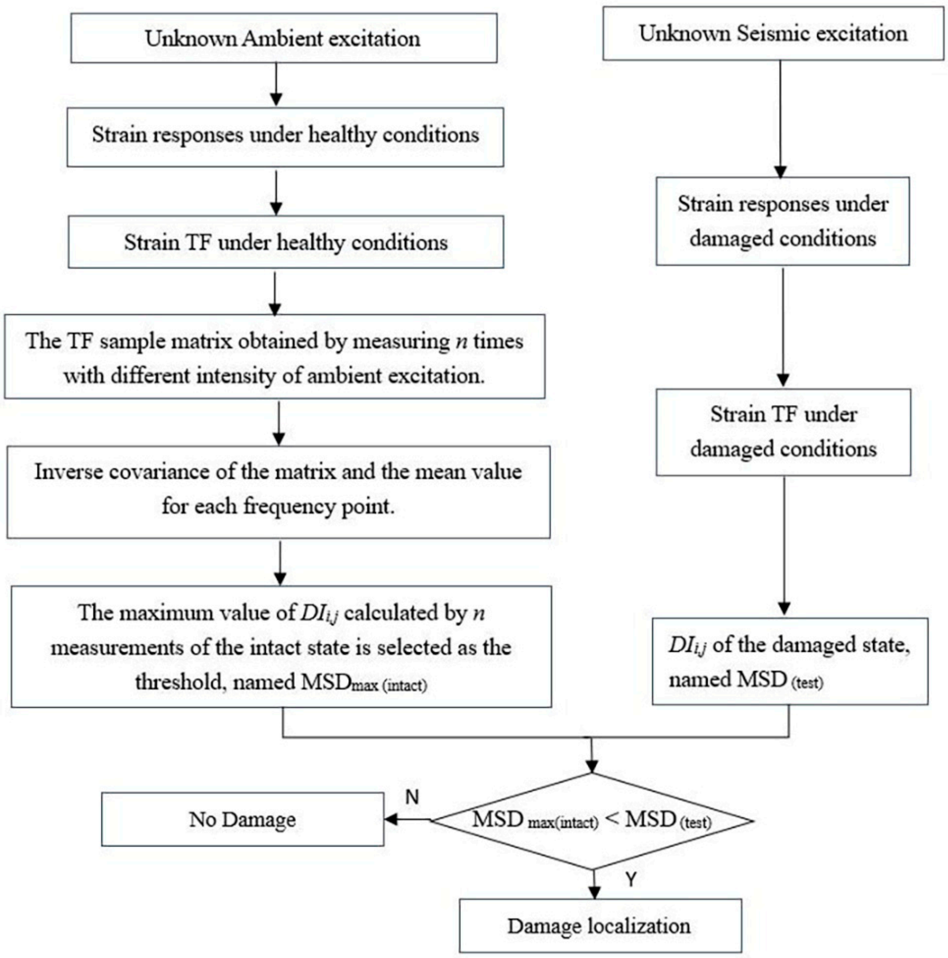

Figure 1. Flowchart of damage localization approach.

4. Numerical Simulation

The numerical simulations of a simply supported beam and a cable-stayed bridge model are carried out to verify the effectiveness of the proposed method. The commercial software MATLAB (2019a) is used to establish the numerical model and process the collected response data.

4.1. Damage Localization of a Simply Supported Beam

As shown in Figure 2, a simply supported beam is used for numerical simulation analysis to verify the proposed method.

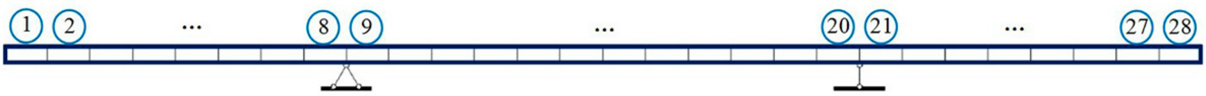

Figure 2. Finite element model of the simply supported beam.

The beam is divided into 28 elements with the element number shown in circles. The length of the beam is 2.8 m (0.1 m for each element). Each member is 9 mm thick and 50 mm wide. The elastic modulus and the mass density of materials are, respectively, 206 GPa and 7800 kg/m^3. Rayleigh damping is adopted for the system with modal damping ratios $\xi_1 = \xi_2 = 0.01$ at the first two modal frequencies. The first six system natural frequencies are 5.51, 8.20, 23.9, 53.7, 62.9, and 82.6 Hz. The strain responses from the 9th element to the 20th element (the middle span of the beam, a total of 12 elements) are measured with sampling frequency of 200 Hz and duration of 30 s. White noise of 30% noise level is added to the observation data, and the noise addition method is: $\varepsilon^m(t) = \varepsilon(t) + Ep \times Noise \times std(\varepsilon(t))$, where $\varepsilon(t)$ is the strain response obtained by simulation calculation, Ep is the noise level, *Noise* is the standard normal distribution random number, and *std* is the standard deviation of $\varepsilon(t)$. Different damage levels are simulated by reducing the stiffness of the beam element.

For the case of the intact structure, Gaussian white noise with the same intensity is applied to each vertical degree of freedom (DOF) of the main beam to simulate the ambient excitation under operating conditions. The same intensity of Gaussian white noise means that their power spectrum is the same; in other words, their second-order statistical properties (including RMS) are the same. For a total of 12 elements, the ninth element is selected as a reference, and the TFs of 11 elements are obtained by Equation (4). Concerning 11 elements, the Fourier transform length here is 2048, and the first 1024 spectral points in each TF imaginary frequency curve are considered. Then, the transmissibility function sample matrix with dimension 500 $\times$ 1024 of the intact structure is obtained by measuring 500 times with different intensities of ambient excitation. The first resonance frequency of the undamaged structure is 5.51 Hz. When MSD is solved, a small frequency band, 3.6–6.5 Hz around the first resonance frequency, that is, 31 frequency points in the first resonance frequency range, is selected for analysis. Finally, the inverse covariance matrix and the mean value of the matrix at each frequency point are obtained.

In the case of a single-element damaged condition, it is assumed that (1) damage occurs in the 17th element with a damage level of 10% subjected to El-Centro earthquake, and (2) damage occurs in the 14th element with a damage level of 10% subjected to Chi-Chi seismic excitation. It is assumed that the El-Centro earthquake and Chi-Chi seismic excitation both act on every vertical DOF. Figure 3a,b show the seismic acceleration records. The TF of each element was calculated by Equation (6) and substituted into Equation (8). Then, the MSD damage indicator of each element is calculated. The results of the damage localization are shown in Figure 4. It is clear that the $\text{MSD}_{(\text{test})}$ in the 17th element and the 14th element significantly exceeds its threshold $\text{MSD}_{\max(\text{intact})}$. Therefore, the 17th element and the 14th element can be detected as damage locations.

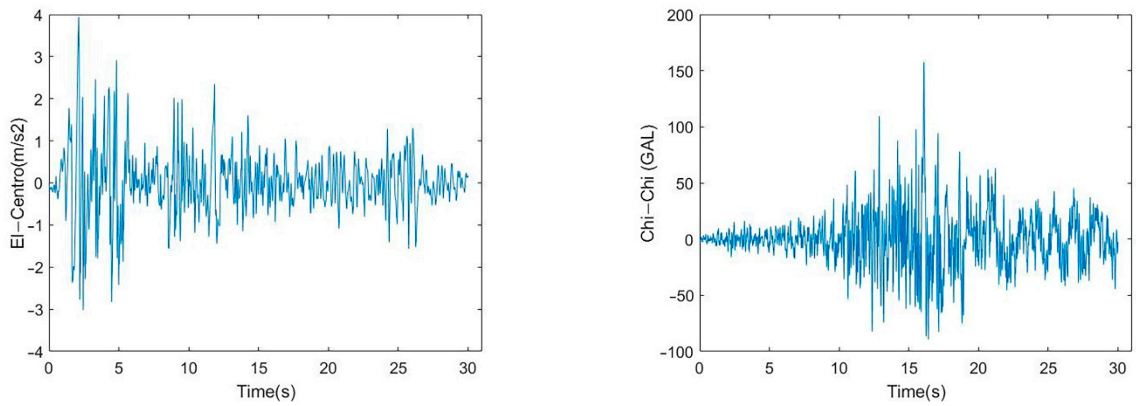

(**a**) (**b**)

Figure 3. (**a**) El-Centro seismic acceleration records; (**b**) Chi-Chi earthquake acceleration records.

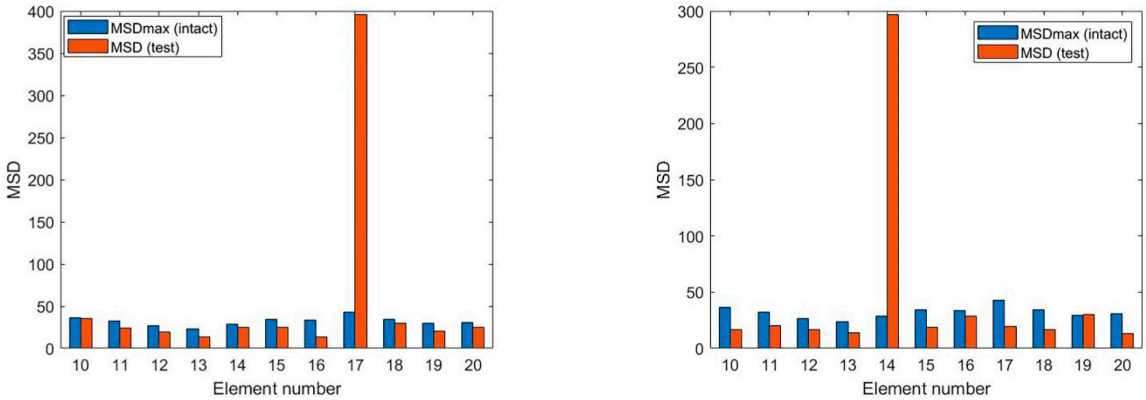

(**a**) (**b**)

Figure 4. (**a**) Single-damage of the 17th element under El-Centro earthquake; (**b**) single-damage of the 14th element under Chi-Chi earthquake.

In the case of multi-element damaged condition, it is assumed that (1) the damage is introduced in the 11th and 17th elements with 10% stiffness reduction under El-Centro earthquake, and (2) the damage is introduced in the 13th element with 10% stiffness reduction and the 18th element with 15% stiffness reduction under Chi-Chi seismic excitation. The results of the damage localization are shown in Figure 5. It is clear that the $MSD_{(test)}$ both in the 11th and the 17th elements and the $MS_{(test)}$ in the 13th and the 18th elements are much greater than their own threshold $MSD_{max(intact)}$. Moreover, the amount by which the $MSD_{(test)}$ exceeds the threshold range of the 18th element is significantly greater than that of the 13th element, which indicates that the damage of the 18th element is more serious.

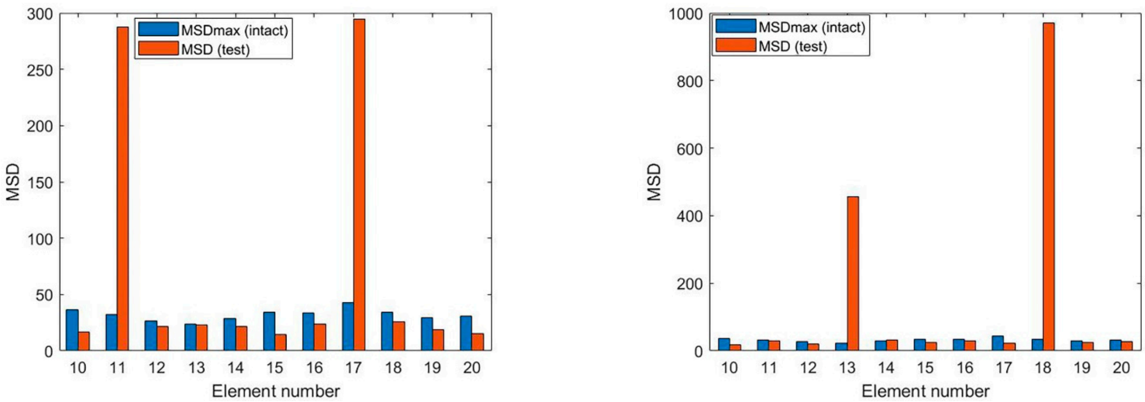

(**a**) (**b**)

Figure 5. (**a**) Multi-damage of the 11th and 17th elements under El-Centro earthquake; (**b**) multi-damage of the 13th and 18th elements under Chi-Chi earthquake.

4.2. Damage Localization of a Cable-Stayed Bridge

The benchmark model of the Puqian Bridge is shown in Figure 6. The length of the main girder of the bridge is 460 m (230 m + 230 m), which is divided into 236 elements. The cables are arranged in a fan shape and divided into 34 elements. The cables are connected to the main girder through motion coupling constraints. The elastic modulus of the cables is corrected by the Ernst formula according to the construction tension cable force. Table 1 summarizes the structural properties of the cable-stayed bridge model. The sampling frequency is 200 Hz, the duration is 30 s, and the strain response is observed at 1/2 of the length of the upper surface of each element. The first six system natural frequencies are 0.315, 0.993, 1.10, 1.52, 1.59, and 1.96 Hz. This paper only studies the linear behaviour of the structure and simulates different degrees of damage by reducing the stiffness of the beam element.

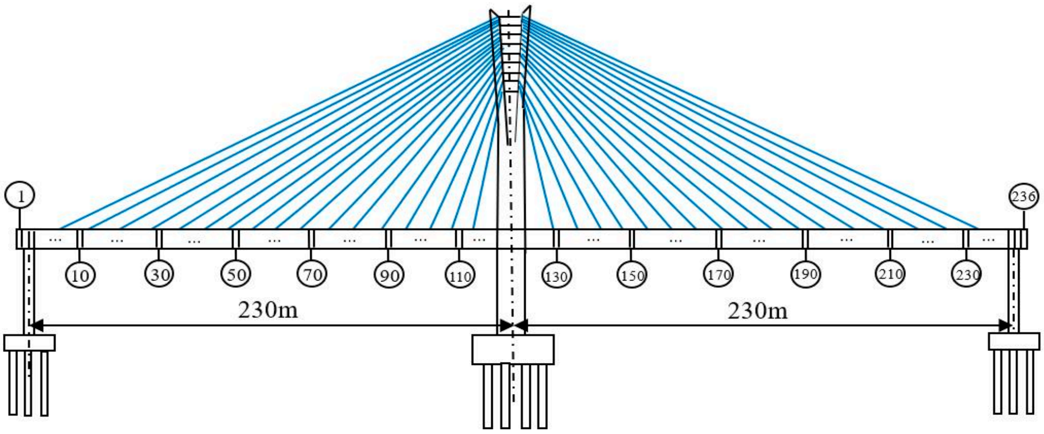

Figure 6. Schematic diagram of a two-dimensional model of a cable-stayed bridge.

Table 1. The main structural parameters of the main bridge.

Beam Properties	Value
Moment of inertia	2.326 m^4
Young's modulus	210 Gpa
Unit length mass	17,555 kg/m
Damping ratio	0.01

For the case of intact structure, Gaussian white noise with the same intensity, that is, the same power spectrum, is applied to each vertical degree of freedom of the main beam to simulate the ambient excitation under operating conditions. Part of the strain responses (from the 50th element to the 70th element) is observed. The time-history of the strain response at the midpoint section of the 69th element is shown in Figure 7a. The white noise of 30% noise level was added to the observation data as the observation response value.

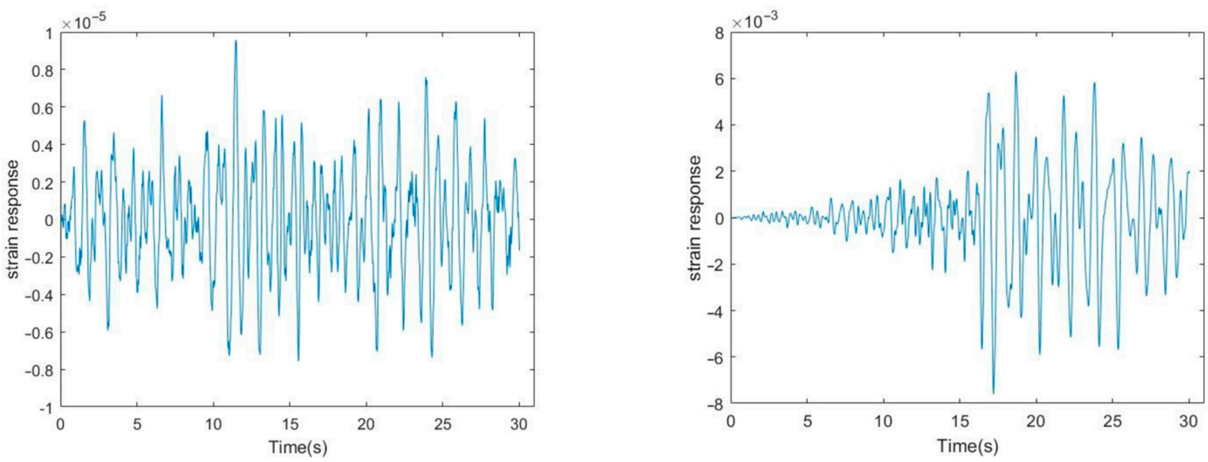

(**a**) (**b**)

Figure 7. (**a**) Time history of strain response in the 69th element under ambient excitation; (**b**) time history of strain response in the 69th element under Chi-Chi earthquake.

The power spectrum of the strain response of the intact structure under ambient excitation is estimated. The 50th element is selected as the reference, and the TF of two measuring points is calculated by Equation (4) as an m-dimensional vector. The Fourier transform length here is 2048. The first 1024 spectral points in the imaginary frequency curve of each TF are considered. Then, a matrix with dimension $n \times m$ is formed by using the method of numerical simulation and repeated observation for n times with different intensities of ambient excitation. After 500 simulations of ambient excitation with different intensities, a dimension of 500×1024 matrix is obtained as the TF matrix of the intact structure. When solving the MSD, 11 frequency points around the first resonance frequency are selected for analysis. Finally, the mean value and inverse covariance matrix is calculated.

For single damage, the damage is introduced with the level of 20% in the 69th element under Chi-Chi earthquake. For multiple damages, the damage level of the 59th element is 15% and that of the 64th element is 20% under Chi-Chi earthquake. It is assumed that Chi-Chi earthquake is applied to every vertical DOF. The numerical simulation response data of the 69th element is shown in Figure 7b, to which Gaussian white noise with a noise level of 30% is added. The results of the damage localization are shown in Figure 8. It is clear that the $\mathrm{MSD}_{(\mathrm{test})}$ of the 69th element is obviously greater than its threshold $\mathrm{MSD}_{\max(\mathrm{intact})}$. Moreover, the $\mathrm{MSD}_{(\mathrm{test})}$ of the 59th element and the 64th element also exceeds its threshold $\mathrm{MSD}_{\max(\mathrm{intact})}$. Similarly, the amount by which the $\mathrm{MSD}_{(\mathrm{test})}$ of the 64th element exceeds the threshold is more than that of the 59th element, indicating that the damage of the 64th element is more serious. Therefore, when there are multiple damages, the degree of damage can be estimated to a certain extent by comparing the $\mathrm{MSD}_{(\mathrm{test})}$ with its threshold value.

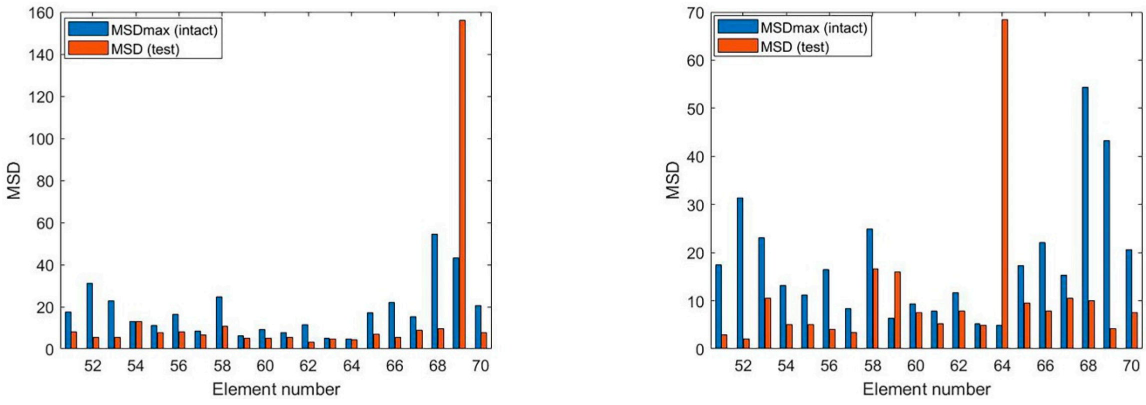

Figure 8. (**a**) Single-damage of the 69th element under Chi-Chi earthquake; (**b**) multi-damage of the 59th and 64th elements under Chi-Chi earthquake.

5. Conclusions

The existing methods for structural damage identification using the TF and MSD are only applied for damage warning. In this paper, an improved method based on MSD of strain TF under unknown seismic excitation is proposed to identify the location of structural damage. The strain TF is employed to eliminate the influence of the unknown seismic excitation and is more sensitive to damage than the traditional TF based on acceleration and displacement data. The fusion of strain TF and MSD is used to extract damage features and identify damage location more effectively. The effectiveness of the method is verified by two numerical simulations of a simply supported beam and a cable-stayed bridge. The results obtained indicate that the proposed method can be used to accurately locate the structural damage with good noise resistance. In addition, in the case of multiple damages, the severity of damage can be estimated tentatively by comparing the degree by which $\mathrm{MSD}_{(\mathrm{test})}$ exceeds its threshold value.

It is noted that the selection of frequency points is based on the experience of selecting points near the resonance frequency. In addition, because bridge structures often exhibit nonlinear behaviors under strong earthquakes, it is necessary to study the detection of their nonlinear behaviors and carry out experimental verification in further research. Moreover, according to engineering experience, the reference sensor should be selected in the place with the smallest damage probability (away from the vulnerable area). In future research, the vulnerability analysis of the structure can be carried out first to determine the location that is not prone to damage. The reference sensor can be arranged at this position, and the influence of different reference sensor positions on the damage localization method can be further studied.

Author Contributions: Conceptualization, X.Z., L.L. and Y.L.; methodology, X.Z. and Y.L.; validation, X.Z. and Y.L.; investigation, X.Z.; data curation, X.Z.; writing—original draft preparation, X.Z.; writing—review and editing, L.L.; funding acquisition, L.L. and Z.Z. All authors have read and agreed to the published version of the manuscript.

Funding: This research was funded by the National Natural Science Foundation of China through Grant No. 52178304 and the National Key R&D Program of China via Grant No. 2017YFC1500603 and Fujian Natural Science Foundation via the Grant No. 2019J01008.

Acknowledgments: The authors also thank Ye Xia of Tongji University for providing the benchmark model of Puqian bridge.

Conflicts of Interest: The authors declare no conflict of interest.

References

1. Rytter, A.; Brincker, R.; Hansen, L.P. Vibration Based Inspection of Civil Engineering Structures. Ph.D. Thesis, Aalborg University, Aalborg, Denmark, 1993.
2. Fan, W.; Qiao, P.Z. Vibration-based damage identification methods: A review and comparative study. *Struct. Health Monit.* **2011**, *10*, 83–111. [CrossRef]
3. Doebling, S.W.; Farrar, C.R.; Prime, M.B. A summary review of vibration-based damage identification methods. *Shock. Vib. Dig.* **1998**, *30*, 91–105. [CrossRef]
4. Li, J.T.; Zhu, X.Q.; Law, S.S.; Samali, B. A two-step drive-by bridge damage detection using dual Kalman filter. *Int. J. Struct. Stab. Dyn.* **2020**, *20*, 2042006. [CrossRef]
5. Xia, Y.; Lei, X.M.; Wang, P.; Sun, L.M. A data-driven approach for regional bridge condition assessment using inspection reports. *Struct. Control Health Monit.* **2021**, *29*, e2915. [CrossRef]
6. Yan, W.J.; Ren, W.X. An Enhanced Power Spectral Density Transmissibility (EPSDT) approach for operational modal analysis: Theoretical and experimental investigation. *Eng. Struct.* **2015**, *102*, 108–119. [CrossRef]
7. Devriendt, C.; Weijtjens, W.; Sitter, G.D.; Guillaume, P. Combining multiple single-reference transmissibility functions in a unique matrix formulation for operational modal analysis. *Mech. Syst. Signal Proc.* **2013**, *40*, 278–287. [CrossRef]
8. Araújo, I.G.; Sánchez, J.A.G.; Andersen, P. Modal parameter identification based on combining transmissibility functions and blind source separation techniques. *Mech. Syst. Signal Proc.* **2018**, *105*, 276–293. [CrossRef]
9. Yan, W.J.; Zhao, M.Y.; Sun, Q.; Ren, W.X. Transmissibility-based system identification for structural health monitoring: Fundamentals, approaches, and applications. *Mech. Syst. Signal Proc.* **2019**, *117*, 453–482. [CrossRef]
10. Chesne, S.; Deraemaeker, A. Damage localization using transmissibility functions: A critical review. *Mech. Syst. Signal Proc.* **2013**, *38*, 569–584. [CrossRef]
11. Meruane, V. Model updating using antiresonant frequencies identified from transmissibility functions. *J. Sound Vibr.* **2013**, *332*, 807–820. [CrossRef]
12. Yan, W.J.; Katafygiotis, L.S. Application of transmissibility matrix and random matrix to Bayesian system identification with response measurements only. *Smart Mater. Struct.* **2016**, *25*, 105017. [CrossRef]
13. Guasch, O.; García, C.; Jové, J.; Artís, P. Experimental validation of the direct transmissibility approach to classical transfer path analysis on a mechanical setup. *Mech. Syst. Signal Proc.* **2013**, *37*, 363–369. [CrossRef]
14. Seijs, M.V.V.D.; Klerk, D.D.; Rixen, D.J. General framework for transfer path analysis: History, theory and classification of techniques. *Mech. Syst. Signal Proc.* **2016**, *68*, 217–244. [CrossRef]
15. Lage, Y.E.; Maia, N.M.M.; Neves, M.M. Force magnitude reconstruction using the force transmissibility concept. *Shock Vib.* **2014**, *2014*, 905912. [CrossRef]
16. Li, X.W.; Zhao, H.T.; Chen, Z.; Wang, Q.B.; Chen, J.A.; Duan, D.P. Force identification based on a comprehensive approach combining Taylor formula and acceleration transmissibility. *Inverse Probl. Sci. Eng.* **2017**, *26*, 1612–1632. [CrossRef]
17. Carrella, A.; Brennan, M.J.; Waters, T.P.; Lopes, V., Jr. Force and displacement transmissibility of a nonlinear isolator with high-static-low-dynamic stiffness. *Int. J. Mech. Sci.* **2012**, *55*, 22–29. [CrossRef]
18. Maia, N.M.M.; Ribeiro, A.M.R.; Fontul, M.; Montalvão, D.; Sampaio, R.P.C. Using the detection and relative damage quantification indicator (DRQ) with transmissibility. *Key Eng. Mater.* **2007**, *347*, 455–460. [CrossRef]
19. Maia, N.M.M.; Almeida, R.A.B.; Urgueira, A.P.V.; Sampaio, R.P.C. Damage detection and quantification using transmissibility. *Mech. Syst. Signal Proc.* **2011**, *25*, 2475–2483. [CrossRef]

20. Zhou, Y.L.; Figueiredo, E.; Maia, N.; Perera, R. Damage detection and quantification using transmissibility coherence analysis. *Shock Vib.* **2015**, *2015*, 290714. [CrossRef]
21. Zhou, Y.L.; Cao, H.Y.; Liu, Q.M.; Wahab, M.A. Output-based structural damage detection by using correlation analysis together with transmissibility. *Materials* **2017**, *10*, 866. [CrossRef] [PubMed]
22. Zhou, Y.L.; Wahab, M.A. Cosine based and extended transmissibility damage indicators for structural damage detection. *Eng. Struct.* **2017**, *141*, 175–183. [CrossRef]
23. Zhou, Y.L.; Maia, N.M.M.; Sampaio, R.P.C.; Wahab, M.A. Structural damage detection using transmissibility together with hierarchical clustering analysis and similarity measure. *Struct. Health Monit.* **2017**, *16*, 711–731. [CrossRef]
24. Chen, J.B.; Diao, Y.S.; Ren, H. Study on structural damage identification based on the transmissibility function. *Struct. Eng.* **2014**, *30*, 32–40. (In Chinese)
25. Al-Jailawi, S.; Rahmatalla, S. Transmissibility-based damage detection using angular velocity versus acceleration. *J. Civ. Struct. Health Monit.* **2018**, *8*, 649–659. [CrossRef]
26. Cheng, L.L.; Cigada, A. An analytical perspective about structural damage identification based on transmissibility function. *Struct. Health Monit.* **2020**, *19*, 142–155. [CrossRef]
27. Luo, Z.W.; Liu, H.L.; Yu, L. Weighted transmissibility assurance criterion for structural damage detection. *J. Aerosp. Eng.* **2021**, *34*, 04021016. [CrossRef]
28. Luo, Z.W.; Liu, H.L.; Yu, L. A multi-state strategy for structural damage detection using sensitivity of weighted transmissibility function. *Int. J. Struct. Stab. Dyn.* **2021**, *21*, 2150144. [CrossRef]
29. Hou, Z.Q. Structural Damage Identification Based on Cosh Spectral Distance and Transmissibility. Master's Thesis, Lanzhou University of Technology, Lanzhou, China, 2016. (In Chinese)
30. Zhou, Y.L.; Figueiredo, E.; Maia, N.; Sampaio, R.; Perera, R. Damage detection in structures using a transmissibility-based Mahalanobis distance. *Struct. Control Health Monit.* **2015**, *22*, 1209–1222. [CrossRef]
31. Zhou, Y.L.; Wahab, M.A. Rapid early damage detection using transmissibility with distance measure analysis under unknown excitation in long-term health monitoring. *J. Vibroeng.* **2016**, *18*, 4491–4499.
32. Chen, J.B. Study on the Structural Damage Identification Based on Acceleration Transmissibility Function. Master's Thesis, Qingdao Technological University, Qingdao, China, 2013. (In Chinese)
33. Zhou, Y.L.; Maia, N.M.M.; Wahab, M.A. Damage detection using transmissibility compressed by principal component analysis enhanced with distance measure. *J. Vib. Control* **2018**, *24*, 2001–2019. [CrossRef]
34. Fan, Z.; Feng, X.; Zhou, J. Structural damage detection by using wavelet based transmissibility function. *Earthq. Eng. Eng. Dyn.* **2014**, *34*, 28–34. (In Chinese)
35. Xu, D.F. Structural Damage Identification of Offshore Platform Based on the Vibration Transmissibility Function and Statistical Hypothesis Testing. Master's Thesis, Qingdao Technological University, Qingdao, China, 2015. (In Chinese)
36. Chen, C.; Wang, Y.H.; Wang, T.; Yang, X.Y. A Mahalanobis distance cumulant-based structural damage identification method with IMFs and fitting residual of SHM measurements. *Math. Probl. Eng.* **2020**, *2020*, 6932463. [CrossRef]
37. Cheng, L.L.; Busca, G.; Roberto, P.; Vanali, M.; Cigada, A. Damage detection based on strain transmissibility for beam structure by using distributed fiber optics. In *Structural Health Monitoring & Damage Detection, Volume 7*; Niezrecki, C., Ed.; Springer: Berlin, Germany, 2017; pp. 27–40.
38. Zhang, X.H.; Zhu, S.; Xu, Y.L.; Homg, X.J. Integrated optimal placement of displacement transducers and strain gauges for better estimation of structural response. *Int. J. Struct. Stab. Dyn.* **2011**, *11*, 581–602. [CrossRef]
39. Shan, D.; Zhou, X.; Yang, J.; Li, Q. Bridge seismic damage identification based on seismic fragility analysis. *J. Vib. Shock* **2017**, *36*, 195–201. (In Chinese)